Journal of Nuclear Materials 115 (1983) 323–330
North-Holland Publishing Company

ELECTRON DAMAGE IN ZIRCONIUM
II. Nucleation and growth of *c*-component loops

M. GRIFFITHS, M.H. LORETTO and R.E. SMALLMAN

Department of Metallurgy and Materials, University of Birmingham, P.O. Box 363, Birmingham B15 2TT, UK

Received 18 October 1982; accepted 8 November 1982

Interstitial loops of $\boldsymbol{b} = \frac{1}{3}\langle 11\bar{2}3\rangle$ have been observed to nucleate and grow during HVEM electron irradiation of Zr at temperatures ~ 650 K. Observations suggest that nucleation and early growth of these loops takes place on a combination of $\{10\bar{1}1\}$ and $\{10\bar{1}0\}$ planes. Subsequent glide of the glissile $\frac{1}{3}\langle 11\bar{2}3\rangle$ dislocations produces irregular loops which lie on irrational planes and are frequently chair-shaped. Of the six possible $\{10\bar{1}1\}$ planes there are only two for which nucleation of these loops is observed in foils having normals close to $\langle 1\bar{2}10\rangle$. These observations and observations of perfect $\langle \boldsymbol{a}\rangle$ type vacancy and interstitial loops have been interpreted in terms of the stress imposed in the Zr foil by the oxide formed during in situ irradiation at high temperature.

The observations are discussed in terms of radiaton-induced growth.

1. Introduction

Dislocation loops having a *c*-component were an integral part of early theories to describe irradiation growth of Zr and its alloys, namely an *a*-axis expansion and a *c*-axis contraction. Buckley's original model [1] for neutron-irradiated Zr proposed that vacancy loops condensed on basal planes (or had a *c*-component) and interstitial loops condensed on prism planes (having $\langle \boldsymbol{a}\rangle$ type Burgers vectors). There have been a few reports of *c*-component loops following neutron irradiation, by Riley and Grundy [2] for example, and following electron irradiation by Gelles and Harbottle [3]. Early observations such as these were based on incomplete analyses and Blake et al. [4] have pointed out that in such cases there was insufficient distinction made between *c*-component damage and thin foil artefacts such as hydrides or oxide. Loops with a *c*-component and of vacancy character have been positively identified, however, by Jostsons et al. [5] but only in two out of five batches of high-purity material and for an irradiation temperature in excess of 723 K. On this basis, one can assume that in the majority of cases only $\langle \boldsymbol{a}\rangle$ type loops nucleate and grow. Experimental observations of the damage microstructure therefore do not support early theoretical predictions relating growth phenomena and dislocation loops. Indeed, even if one assumes that the loops observed in growth specimens were oriented so as to give maximum growth strain, recent evidence shows that, for polycrystalline material at least, the magnitude of the growth strain cannot be accounted for by the number and size of loops [6].

Carpenter et al. [7], have irradiated single-crystal Zr specimens at low temperature (< 553 K) and their results show a clear *a*-axis expansion and a *c*-axis contraction. Because of the small size of loops at these temperatures there is no TEM evidence as to their character. Carpenter suggests that the growth is due to submicroscopic defects such as small vacancy loops or clusters as well as a large number of observed $\langle \boldsymbol{a}\rangle$ type loops presumed to be interstitial. With these assumptions it is possible that Buckley's theory can explain the experimental observations of growth strain. This model cannot, however, account either for measured growth strains at higher temperatures or for the growth in polycrystalline material, both because the total loop density is inadequate to account for the growth and because vacancy loops of $\boldsymbol{b} = \frac{1}{3}\langle 11\bar{2}0\rangle$ are observed rather than *c*-component vacancy loops.

Grain boundaries and initial dislocation density clearly play an important role in irradiation growth. Dollins [8] has performed numerous calculations to predict growth strain in Zr in various metallurgical states. He assumes that growth comes from four sources: (1) preferred nucleation and growth of interstitial dislocation loops, (2) climb of network dislocations with preferred Burgers vectors, (3) depleted zone formation, and (4) point-defect absorption at sub-grain boundaries.

0022-3115/83/0000–0000/$03.00

He obtains quite good agreement with experimental observations for a temperature of 575 K and concludes that growth is primarily due to the climb of network dislocations in cold-worked materials and to nucleation and growth of interstitial dislocation loops in annealed material. Carpenter and Northwood [6] have clearly shown, however, that for annealed material at 575 K the strain calculated from the observed dislocation loops is far lower than the measured growth strain. In more recent models such as those of MacEwen and Carpenter [9] no account is taken of the contribution to growth from dislocation loops because such a contribution is known to be small and effective only for a short transient period at low damage levels. They consider polycrystalline Zr of various degrees of cold work for fixed conditions of material texture and grain shape. The basis of their models is the partitioning of point defects to network dislocations and grain boundaries. This partitioning is influenced by such factors as pipe diffusion of vacancies along screw dislocations, radiation-enhanced recovery of the network and the relative mobility of interstitials and vacancies, which is in turn influenced by solute trapping and the mobility of divacancies. Essentially, growth is enhanced for a high network dislocation density and small grain size and occurs to a greater or lesser extent as the sink efficiency of the network for vacancies is varied. Although models such as these can reasonably predict growth strains for cold-worked materials there remains no adequate explanation for irradiation-growth in a well annealed material. Models, such as that of Yoo [10], developed to explain the suppression of void formation in Zr, based on an internal stress mechanism, could provide an explanation for growth. Internal stresses exist in polycrystalline material as a result of temperature changes, interstitial gaseous impurities and radiation damage (in the form of Frenkel pairs or climbing dislocations). Yoo has shown that the distortion of the lattice by thermal expansion and the dissolved interstitial gas atoms is greater parallel with the *c*-axis than that parallel with the *a*-axis and the resultant stress in a constrained grain can be relieved by deposition of vacancies on grain boundaries perpendicular to the *c*-axis and interstitials perpendicular to the *a*-axis. Moreover, a hydrostatic stress field can be relieved by deposition of point defects in the same manner.

Clearly, at temperatures for which the vacancies are relatively immobile the formation of interstitial $\langle a \rangle$ type loops will contribute to the lattice expansion in this direction. At higher temperatures ~ 675 K, however, for which approximately equal numbers of vacancy and interstitial $\langle a \rangle$ type loops have been observed [4], it is unlikely that there is any net contribution to the growth from the loops unless there is some degree of crystallographic partitioning in the basal plane related to the loop character. A study of point-defect behaviour in forming clusters over a wide temperature range is necessary to further the understanding of radiation enhanced growth and swelling processes.

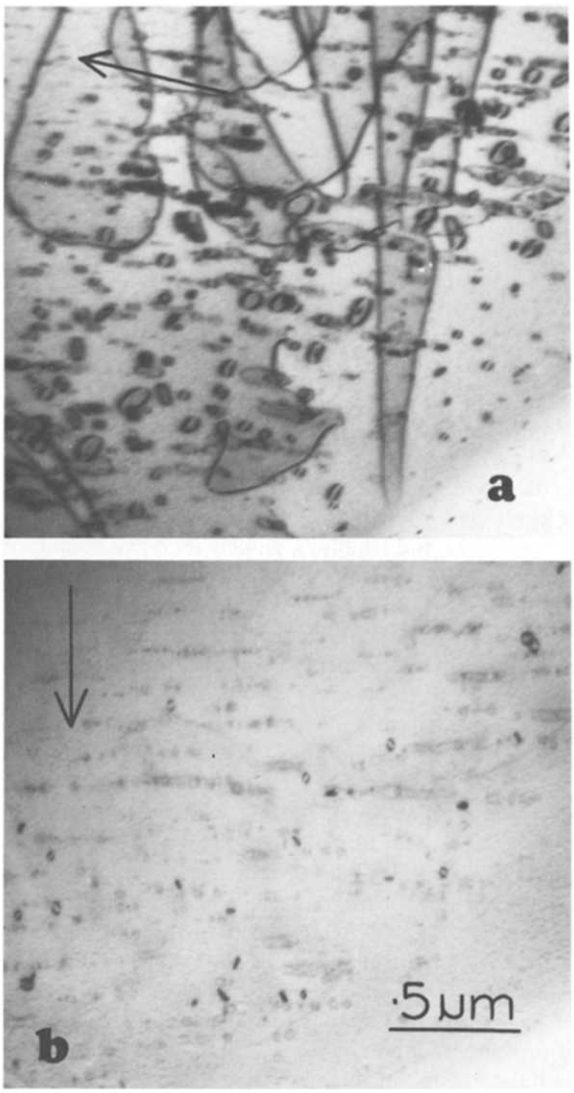

Fig. 1. Imaging of *c*-component loops in Zr following electron irradiation at ~ 675 K to ~ 0.1 dpa. The $\langle a \rangle$ type damage shows zero contrast with a $000\bar{4}$ diffracting vector whereas *c*-component damage (in this case having $\boldsymbol{b} = \frac{1}{3}\langle 11\bar{2}3 \rangle$) shows up clearly interspersed among the layers by $\langle a \rangle$ type loops; (a) $\boldsymbol{g} = \bar{2}110$, $\boldsymbol{B} \sim [0\bar{1}10]$, (b) $\boldsymbol{g} = 000\bar{4}$, $\boldsymbol{B} \sim [1\bar{2}10]$.

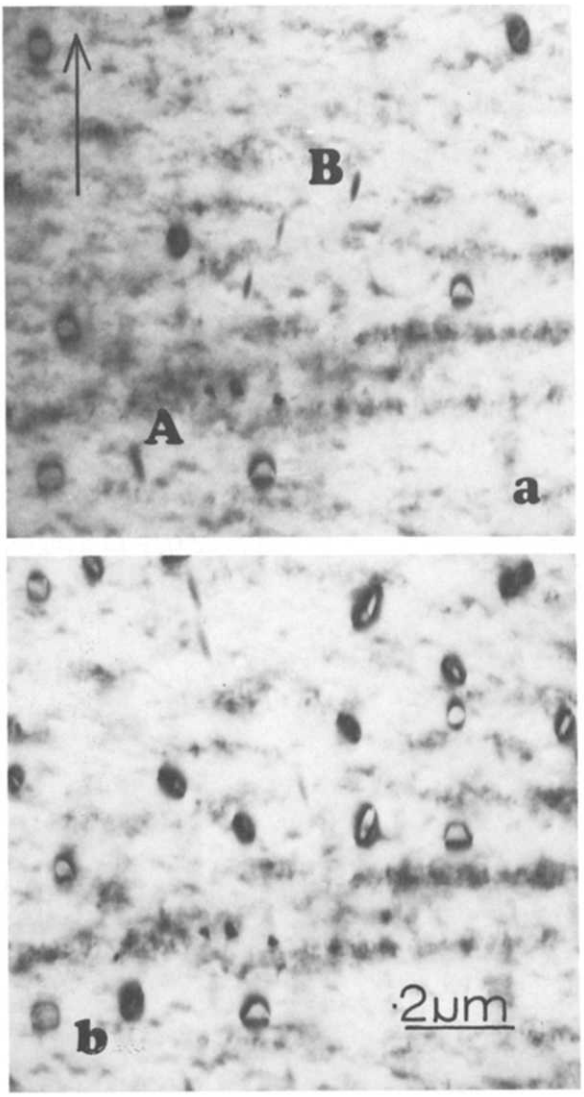

Fig. 2. Nucleation of c-component loops in Zr during electron irradiation at ~ 675 K. Loops A and B nucleate on planes containing $\boldsymbol{B} = [1\bar{2}10]$ and correspond to the $(10\bar{1}1)$ and $(\bar{1}011)$ planes respectively, $\boldsymbol{g} = 000\bar{4}$, $\boldsymbol{B} \sim [1\bar{2}10]$; (a) 0.10 dpa, (b) 0.12 dpa.

Carpenter and Watters [11] have reported that c-component loops are not formed during electron irradiation at least for moderate doses up to 1 dpa. They have observed defects having a c-component strain field, however, for doses in excess of 10 dpa at 580 K. There may be some correlation between these defects and the large faulted basal defects observed following neutron irradiation of 64% cold-worked Ti at equivalent temperatures and damage levels [12].

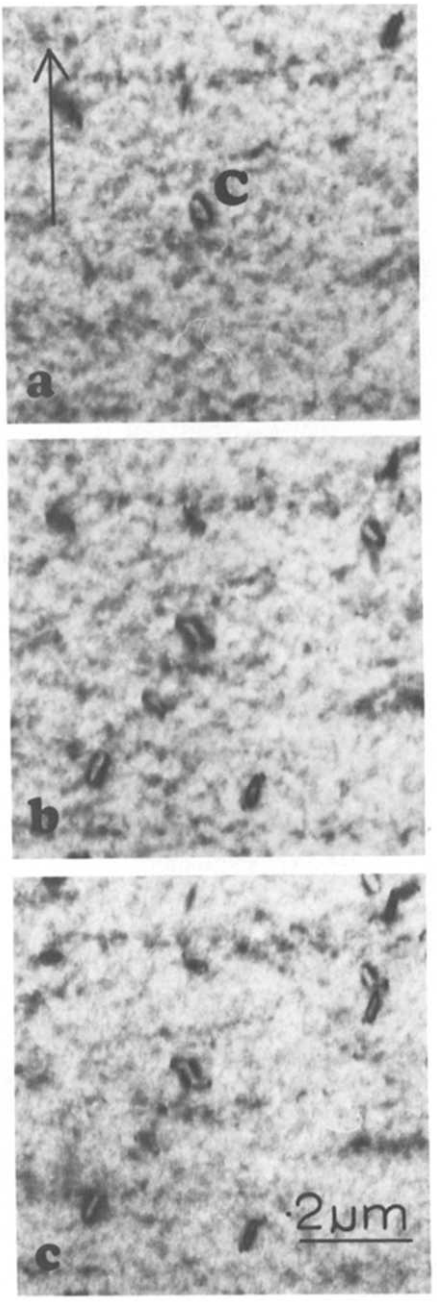

Fig. 3. Climb and glide of loops having $\boldsymbol{b} = \frac{1}{3}\langle 11\bar{2}3\rangle$ during electron irradiation of Zr at ~ 725 K. Loop C grows into an irregular chair-shape after rotating from its initial nucleation plane, $\boldsymbol{g} = 000\bar{4}$, $\boldsymbol{B} \sim [1\bar{2}10]$; (a) 0.06 dpa, (b) 0.08 dpa, (c) 0.12 dpa.

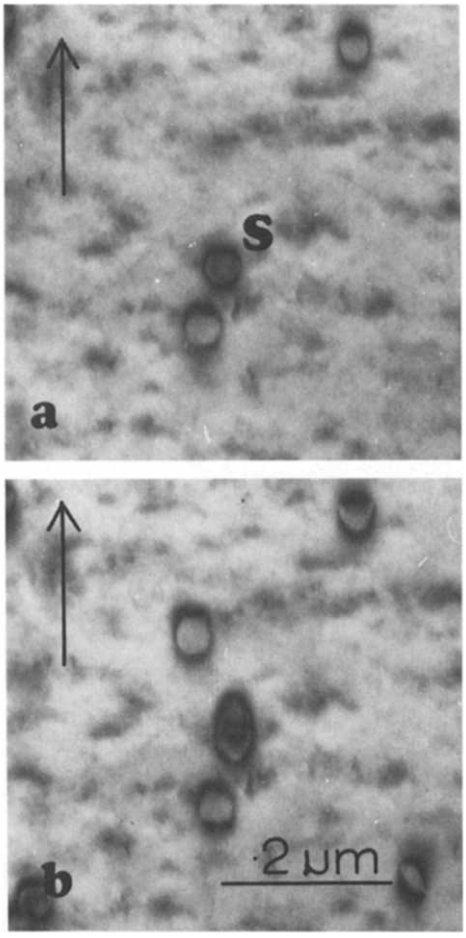

Fig. 4. Splitting of complex double loops during electron irradiation of Zr at ~ 675 K. Loop S has a *c*-component Burgers vector and is comprised of two concentric loops. Splitting is enhanced as the growth of the outer component occurs in preference to the inner, $\boldsymbol{g} = 000\bar{4}$, $\boldsymbol{B} \sim [1\bar{2}10]$; (a) 0.08 dpa, (b) 0.12 dpa.

The present work has been undertaken to investigate more fully the enigma of the *c*-component loop by in situ irradiation of Zr in a HVEM and hence to assess its possible role in irradiation-growth.

2. Experimental

Experimental procedures are outlined in paper I [13].

3. Results

Dislocation loops having a *c*-component have been observed for a range of temperatures between 575–775 K during electron irradiation in the present work. Perfect loops of $\boldsymbol{b} = 1/3\langle 11\bar{2}3\rangle$ or $\langle \boldsymbol{c} + \boldsymbol{a}\rangle$ are the most

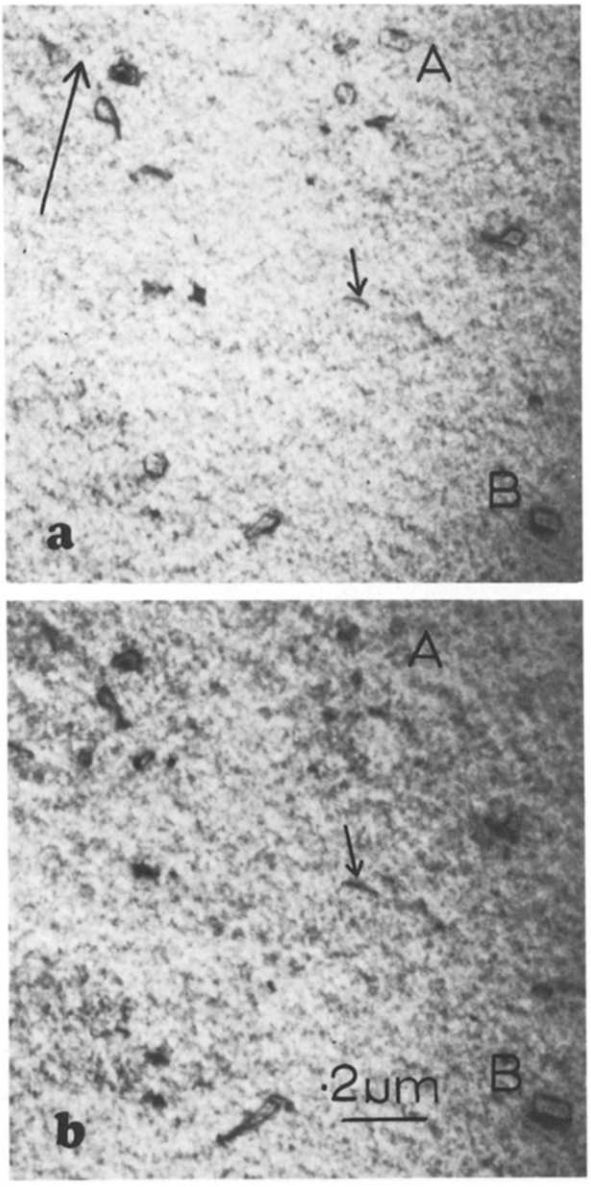

Fig. 5. Growth of *c*-component loops during electron irradiation of Zr at ~ 775 K. Loop A appears to shrink whereas loop B appears to grow, $\boldsymbol{g} = 000\bar{4}$, $\boldsymbol{B} \sim [1\bar{2}10]$; (a) 0.08 dpa, (b) 0.14 dpa.

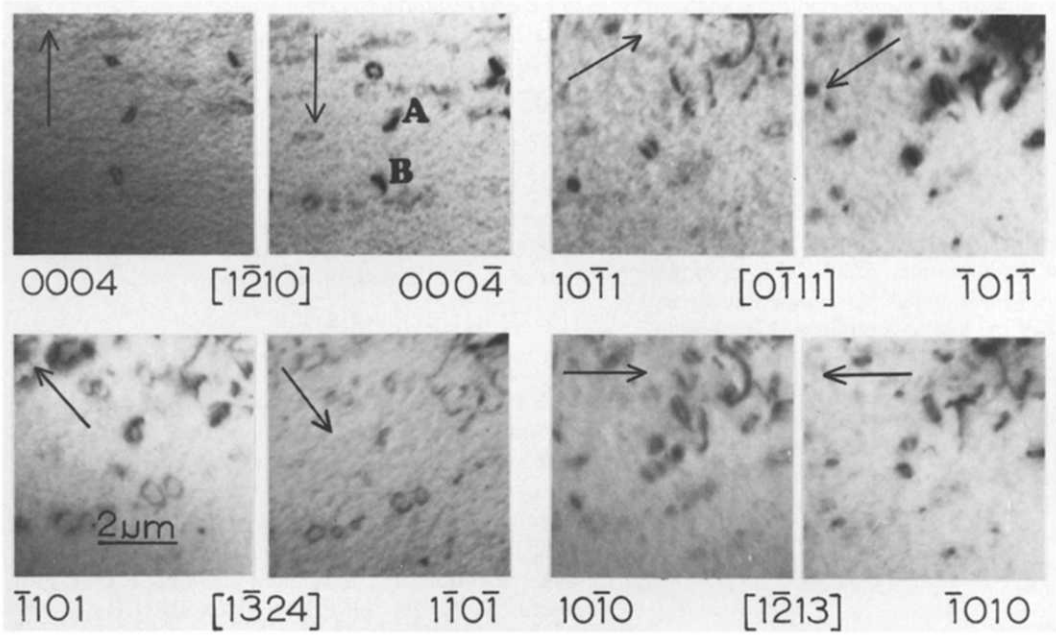

Fig. 6. Characterisation of *c*-component dislocation loops in Zr following electron irradiation at ~ 675 K. Loop A has $\boldsymbol{n} \sim [\bar{1}\bar{1}23]$, $\boldsymbol{b} = \frac{1}{3}[\bar{1}\bar{1}23]$ and loop B has $\boldsymbol{n} \sim [2\bar{1}\bar{1}3]$, $\boldsymbol{b} = \frac{1}{3}[2\bar{1}\bar{1}3]$ and both are interstitial in nature, $\boldsymbol{g}$ and $\boldsymbol{B}$ are indicated for each figure.

common *c*-component defects observed. In one case, for a very low irradiation dose and a heavily oxidised sample, small loops (~ 200 Å diameter) have been observed having Burgers vectors of $\boldsymbol{b} = 1/6\langle 20\bar{2}3\rangle$ [14]. The *c*-component loops are distinguished from and are observed between the layers of $\langle \boldsymbol{a} \rangle$ type damage using a 0004 diffracting vector, (fig. 1). Increasing irradiation temperature leads to a decrease in loop density and an increase in the size of the loops for a given dose rate.

At irradiation temperatures below 500 K analysis was not practicable because of the high density and close banding of the $\langle \boldsymbol{a} \rangle$ type damage. This high density of loops severely distorts the crystal and although contrast is observed when attempting to image with a 0004 diffracting vector it can be accounted for in terms of crystal distortion and the absence of two-beam imaging conditions. At higher irradiation temperatures, the $1/3\langle 11\bar{2}3\rangle$ loops are observed on planes which contain $\langle 1\bar{2}10\rangle$ and are inclined to (0001) and $\{10\bar{1}0\}$, which is consistent with nucleation and early growth on a combination of $\{10\bar{1}1\}$ and $\{10\bar{1}0\}$ planes. Because of the *c*-component in the loop Burgers vector, the nucleation plane will be assumed to be $\{10\bar{1}1\}$.

In the case of foils near $\langle 1\bar{2}10\rangle$, nucleation has been observed on only two of the six possible $\{10\bar{1}1\}$ planes. These planes are those most nearly perpendicular to the foil surface. Fig. 2 illustrates an irradiation sequence at 675 K. Loops A and B can be seen to have nucleated on planes containing $\boldsymbol{B} \sim [1\bar{2}10]$ which correspond to the $(10\bar{1}1)$ and $(\bar{1}011)$ planes respectively. When the loops have reached a certain critical size, which is a function of temperature, foil thickness, degree of oxidation etc, they rotate by glide to more energetically stable orientations. Further growth and glide frequently results in complex chair-shaped loops as illustrated in fig. 3 for an irradiation at 725 K. In some cases double loops have been observed, the degree of splitting increasing with continued irradiation. The loop marked S in fig. 4 is one example of this.

Fig. 5 shows that loop nucleation has effectively saturated at 775 K and that some loops shrink (loop A) while others grow (loop B). Although it is not possible to distinguish between climb and glide under these conditions, it has already been observed that glide generally results in complex chair-shaped loops which is clearly not the case in this example. It is assumed therefore that the size changes shown in fig. 5 are the result of climb. A small number of defects, which may be loops, appear to lie on the basal plane (arrowed) but none of these defects has been analysed.

Only a small number of loops could be analysed because of difficulties encountered with asymmetric image contrast [15] and the high density of $\langle a \rangle$ type loops comprising ~ 90% of the total loop population. Analysis of loops following irradiation at 675 K is illustrated in fig. 6. The loop marked A is out of contrast with $\boldsymbol{g} = 10\bar{1}1$ and is in contrast with $\boldsymbol{g} = 10\bar{1}0$. It exhibits outside contrast with $\boldsymbol{g} = 0004$ and $\boldsymbol{g} = \bar{1}101$ and therefore has $\boldsymbol{b} = 1/3[\bar{1}\bar{1}23]$. It has $\boldsymbol{n} \sim [\bar{1}\bar{1}23]$ and is therefore interstitial in nature. Similarly loop B has $\boldsymbol{b} = 1/3[2\bar{1}\bar{1}3]$, $\boldsymbol{n} \sim [2\bar{1}\bar{1}3]$ and is also interstitial in nature. Only ~ 10% of the total c-component loop population has been analysed in this manner with any degree of confidence. No vacancy $\langle c + a \rangle$ loops have been found although it cannot be proved that they are absent from the foil on the basis of the analysing only ~ 10% of the total. Because of the similarity in nucleation planes and loop behaviour, however, it will be assumed for the purposes of the following discussion that all loops having $\boldsymbol{b} = 1/3\langle 11\bar{2}3 \rangle$ are interstitial in nature.

4. Discussion

4.1. Nucleation and growth of c-component loops in electron irradiated Zr

The observations in fig. 2 show that c-component loops appear to lie on two planes, approximating to $(30\bar{3}2)$ and $(\bar{3}032)$, from the stage at which they are first visible, many of them rotating during growth to form complex-shaped loops. Nucleation presumably occurs on either $\{10\bar{1}0\}$ or $\{10\bar{1}1\}$ with subsequent addition of atoms along the shortest bond distance, $1/6\langle 20\bar{2}3 \rangle$, so that the initial plane on which nucleation occurs is no longer apparent.

Insertion of an extra plane of atoms on $\{10\bar{1}0\}$ to give rise to a c-component loop seems very unlikely since the c-component would clearly have to originate from the subsequent shear and the required shear can be seen, from a ball model, to be most improbable. It is in fact much more likely that nucleation on $\{10\bar{1}0\}$ would lead to an $\langle a \rangle$ type loop by the following reaction:

$$\tfrac{1}{2}[\bar{1}010] \xrightarrow[\text{on } (10\bar{1}0)]{\frac{1}{6}[\bar{1}2\bar{1}0]} \tfrac{1}{3}[\bar{2}110].$$

On the above basis, it seems likely that the nucleation of c-component loops occurs on $\{10\bar{1}1\}$ and various reactions are possible involving either the insertion of a single plane of atoms followed by a shear with a significant c-component or the successive insertion of two planes of atoms. Considering first the insertion of only one plane of atoms to give a faulted loop of $\boldsymbol{b} = \frac{1}{9}[5\bar{3}\bar{2}3]$ or $\frac{1}{6}[20\bar{2}3]$ followed by shear, we can write for condensation on $(10\bar{1}1)$:

$$\tfrac{1}{9}[5\bar{3}\bar{2}3] + \tfrac{1}{18}[2\bar{6}43] + \tfrac{1}{6}[\bar{2}023] \rightarrow \tfrac{1}{3}[1\bar{2}13] \qquad (1)$$

or $\frac{1}{6}[20\bar{2}3] + \frac{1}{6}[\bar{2}023] \rightarrow [0001]$.

These loops have a very high shear component ($\sim 60°$) and it should be noted that alternative shears, which are energetically more favourable, can result in the generation of the $\langle a \rangle$ type loop as follows:

$$\tfrac{1}{9}[5\bar{3}\bar{2}3] + \tfrac{1}{9}[10\bar{1}\bar{3}] \rightarrow \tfrac{1}{3}[2\bar{1}\bar{1}0]$$

or $\frac{1}{6}[20\bar{2}3] + \frac{1}{18}[4\bar{6}\bar{2}3] + \frac{1}{9}[10\bar{1}\bar{3}] \rightarrow \frac{1}{3}[2\bar{1}\bar{1}0]$.

Thus the insertion of only one plane is likely to result in the formation of an $\langle a \rangle$ type loop rather than c-component loop. It may be possible that a shear stress acting so as to displace the inserted plane of atoms in a direction acute to [0001] or $[1\bar{2}13]$ will cause reaction (1) to take place. It is conceivable that such stresses exist under the thin foil irradiation conditions previously described. In view of the fact that the c-component loops are all glissile and [0001] dislocations are believed to be sessile the final displacement is most likely to be $1/3[1\bar{2}13]$ in this case.

Considering next the successive insertion of two planes of atoms the following reaction is possible on $(10\bar{1}1)$:

$$\tfrac{1}{6}[20\bar{2}3] + \tfrac{1}{6}[02\bar{2}3] \rightarrow \tfrac{1}{3}[11\bar{2}3]. \qquad (3)$$

(1st layer)(2nd layer)

The formation of loops of $\boldsymbol{b} = 1/3\langle 11\bar{2}3 \rangle$ thus looks to be a reasonable possibility if the initial nucleation event is the formation of a faulted loop of $\boldsymbol{b} = 1/6\langle 20\bar{2}3 \rangle$. Subsequent condensation of the appropriate $1/6\langle 02\bar{2}3 \rangle$ loop unfaults the initial loop and hence allows glide to give a loop of more edge character. This mechanism is consistent with the observation of $1/6\langle 20\bar{2}3 \rangle$ loops at low doses, although it should be emphasised that these were observed only once and their character was not determined. Further, it is consistent with the observation of double loops (fig. 4) which were occasionally observed and it is therefore concluded that the nucleation and growth of $\langle c + a \rangle$ loops is most adequately described by this latter mechanism.

The fact that point defects condense on only two out of the six possible $\{10\bar{1}1\}$ planes for prism foils suggests that the nucleation of $\langle c + a \rangle$ loops is influenced by some external factor i.e., the nucleation is not entirely governed by the crystallography of Zr. These observations together with the data from analysis of the $\langle a \rangle$

type loops [13] suggest that a stress-relief mechanism is determining the nucleation of the damage. The most likely source of such a stress is that which arises from the oxidation of the thin foil during high temperature irradiation. For a material such as Zr, having a coherent oxide which grows with a volume expansion, compressive stresses will exist in the oxide. Corresponding tensile stresses in the metal will be in the plane of the foil. This stress distribution is entirely consistent with observations of the $\langle a \rangle$ type and *c*-component damage in which vacancy loops tend to condense on planes as closely parallel as possible with the foil surface and interstitial loops condense on planes as closely perpendicular to the foil surface as possible. Oxide thicknesses in the present work have been measured using Auger spectroscopy to be ~ 500 Å following irradiation at 675 K. Typical compressive stresses in a growing oxide are of the order of 0.4 GN m^2 and from this a lower-bound estimate for tensile stresses in a foil of 3000 Å thickness is ~ 0.05 GN m^2 which is of the same order of magnitude as the yield stress of Zr. The energy of the system can be lowered as a result of the nucleation and growth of suitably oriented interstitial and vacancy loops with respect to this stress.

Assuming that the formation energies for vacancies and interstitials are 1.6 and 4 eV respectively and that 4 point defects constitute a stable loop nucleus, then it is possible to estimate the chemical stress for which loop nucleation will occur during irradiation. This value is ~ 1.3 GN m^2 for both interstitial and vacancy loops and is clearly very much greater than typical oxide-induced stresses in the foil of ~ 0.05 GN m^2. Thus the stress-induced preferential nucleation mechanism (SIPN) is unlikely to be significant in determining loop behaviour. The stress-induced preferential absorption (SIPA) of point defects at existing loops is possibly more significant. The energy of the system can be lowered by vacancy loops growing parallel with, and interstitial loops growing perpendicular to, a tensile stress.

For example, the bias of an edge dislocation for interstitials increases by ~ 0.5% when the dislocation Burgers vector is parallel as compared with perpendicular to the tensile stress axis in the foil and vice-versa for vacancies, although the change in bias is sligthly higher for the vacancy interaction.

The fact that the majority of *c*-component loops have $\boldsymbol{b} = \frac{1}{3}\langle 11\bar{2}3 \rangle$ and nucleate on $\{10\bar{1}1\}$ planes, at least for prism foils, is perhaps a little surprising. There are a few examples of defects (arrowed in fig. 5) which are believed to be loops and appear to have nucleated on the basal plane but in general such loops are uncommon. Although the basal plane is slightly more close-packed than the $\{10\bar{1}1\}$ planes, loops nucleating on $\{10\bar{1}1\}$ are more effective in relieving what amounts to a radial stress in the foil and this could explain their predominance. It is conceivable, however, that impurities in the foil can change the local spacings and thus favour the nucleation of loops on $\{10\bar{1}1\}$ as opposed to (0001). This mechanism has been proposed by Jostsons et al. [16] in explaining the nucleation of faulted vacancy loops on (0001) in some of their neutron irradiated samples. The results of Jostsons et al. show that only samples having a high interstitial gas content produced basal vacancy loops. The condensation of vacancies to form these loops is consistent in relieving an internal compressive stress parallel with the *c*-axis which results from the solution of gaseous impurities [10]. In such cases one can describe the defect behaviour as stress or impurity driven because the two mechanisms are indistinguishable.

If one assumes that the loops formed during electron irradiation are a product of the unusual stress conditions then factors such as edge character and stacking fault energy become less significant in determining loop plane. The important factor is the orientation of the stress field which is determined by the plane of the foil. The fact that higher energy $\langle c + a \rangle$ loops are all interstitial whereas $\langle a \rangle$ loops are either interstitial or vacancy may reflect either the higher driving force for interstitial loop formation or the fact that the nucleation paths in the formation of a vacancy or interstitial $\langle c + a \rangle$ loops are very different.

4.2. Comparison with neutron irradiation and the role of c-component loops in irradiation growth

It has already been established in the introduction that dislocation loops do not contribute significantly to the macroscopic growth of irradiated specimens, growth occurring mainly as a result of the absorption of point defects at network dislocations and grain boundaries. Although the *c*-component loop is historically important in accounting for a *c*-axis contraction of Zr during irradiation it would appear from the results presented here that the nucleation, growth and character of *c*-component loops is governed to a large extent by a stress in the matrix. The observations of Jostsons et al. [16] of basal vacancy loops in neutron irradiated Zr have already been discussed in terms of the influence of an internal stress arising from dissolved gaseous impurities. In other materials, also, there is unequivocal evidence to show that stresses strongly influence loop behaviour. For example, Brager et al. [17] have shown

that in neutron-irradiated 316 stainless steel the total area of Frank interstitial loops increases five-fold for loop orientations perpendicular to a resolved tensile stress of ~ 0.3 GN m^2. On this basis the effect of internal stresses on the morphology of dislocation loops must always be taken into account when assessing the contribution of these loops to be growth of the material. Indeed, variations in internal stresses could account for the wide variation in distribution of vacancy and interstitial loops from grain to grain sometimes observed in neutron irradiated Zr [18].

The results presented here give evidence to support the view that the irradiation growth of Zr is not directly a result of the formation of *c*-component vacancy loops. Stresses can influence dislocation loop nucleation and growth and must be considered when describing dislocation loop structures formed during irradiation. Further work involving a variation of foil normals during electron irradiation is in the process of completion and will be presented in a future publication.

5. Conclusions

(1) *c*-component loops having Burgers vectors of $\boldsymbol{b} = \frac{1}{6}\langle 20\bar{2}3\rangle$ and $\frac{1}{3}\langle 11\bar{2}3\rangle$ nucleate and grow during electron irradiation of Zr.

(2) Loops of $\boldsymbol{b} = \frac{1}{3}\langle 11\bar{2}3\rangle$ are interstitial in nature and nucleate on non-basal planes.

(3) Oxidation of thin foils during high-temperature electron irradiation results in stresses which influence loop growth. Interstitial and vacancy loops grow preferentially on planes respectively perpendicular and parallel to a tensile stress.

Acknowledgements

We would like to acknowledge SERC support in the form of a studentship for one of us (M.G.) and for financial support for the HVEM under grant number GR/B/30371. We would also like to acknowledge I.P. Jones and J. White for many useful discussions and I. Alexander for Auger spectrometry work.

References

[1] S.N. Buckley, in: Properties of Reactor Materials and Effects of Radiation Damage, Ed. D.J. Littler (Butterworth, London, 1962) p. 413.
[2] A. Riley and P.J. Grundy, Phys. Status Solidi (a)14 (1972) 239.
[3] D.S. Gelles and J.E. Harbottle, CEGB report RD/B/N2973 (1974).
[4] R.G. Blake, A. Jostsons and P.M. Kelly, AAEC/E374 (1976).
[5] A. Jostsons, R.G. Blake, J.G. Napier, P.M. Kelly and K. Farrell, J. Nucl. Mater. 68 (1977) 267.
[6] G.J.C. Carpenter and D.O. Northwood, J. Nucl. Mater. 56 (1975) 260.
[7] G.J.C. Carpenter, R.A. Murgatroyd, A. Rogerson and J.F. Watters, J. Nucl. Mater. 101 (1981) 28.
[8] C.C. Dollins, J. Nucl. Mater. 59 (1975) 61.
[9] S.R. MacEwen and G.J.C. Carpenter, J. Nucl. Mater. 90 (1980) 108.
[10] M.H. Yoo, Zirconium in Nuclear Applications, ASTM-STP-511 (1974) 292.
[11] G.J.C. Carpenter and J.F. Watters, J. Nucl. Mater. 96 (1981) 213.
[12] M. Griffiths and D. Faulkner, unpublished work.
[13] M. Griffiths, M.H. Loretto and R.E. Smallman, Electron damage in zirconium I, preceeding article in this issue.
[14] M. Griffiths, R.E. Smallman and M.H. Loretto, Proc. 6th Intern. Conf. on HVEM, Antwerp (1980) p. 220.
[15] M. Griffiths, J. White, R.E. Smallman, M.H Loretto and I.P. Jones, Proc. 10th Intern. Congress on Electron Microscopy, Hamburg (1982).
[16] A. Jostsons, P.M. Kelly and R.G. Blake, 9th ASTM Intern. Symp. on Effects of Radiation Damage in Structural Materials, ASTM-STP-683 (1978) 46.
[17] H.R. Brager, F.A. Garner and G.L. Guthrie, J. Nucl. Mater. 66 (1977) 301.
[18] A. Jostsons, P.M. Kelly and R.G. Blake, J. Nucl. Mater. 66 (1977) 236.